

Liposome-based Formulation for Intracellular Delivery of Functional Proteins

Benoît Chatin, Mathieu Mével, Julie Devallière, Laurence Dallet, Thomas Haudebourg, Pauline Peuziat, Thibault Colombani, Mathieu Berchel, Olivier Lambert, Aleksander Edelman, et al.

▶ **To cite this version:**

Benoît Chatin, Mathieu Mével, Julie Devallière, Laurence Dallet, Thomas Haudebourg, et al.. Liposome-based Formulation for Intracellular Delivery of Functional Proteins. Molecular Therapy - Nucleic Acids, 2015, 4, 10.1038/mtna.2015.17 . hal-01537608

HAL Id: hal-01537608
https://hal.univ-brest.fr/hal-01537608

Submitted on 11 Jul 2018

HAL is a multi-disciplinary open access archive for the deposit and dissemination of scientific research documents, whether they are published or not. The documents may come from teaching and research institutions in France or abroad, or from public or private research centers.

L'archive ouverte pluridisciplinaire **HAL**, est destinée au dépôt et à la diffusion de documents scientifiques de niveau recherche, publiés ou non, émanant des établissements d'enseignement et de recherche français ou étrangers, des laboratoires publics ou privés.

Citation: Molecular Therapy—Nucleic Acids (2015) 4, e244; doi:10.1038/mtna.2015.17
© 2015 The American Society of Gene & Cell Therapy All rights reserved 2162-2531/15
www.nature.com/mtna

Liposome-based Formulation for Intracellular Delivery of Functional Proteins

Benoît Chatin[1,2], Mathieu Mével[1,2], Julie Devallière[1,2], Laurence Dallet[3], Thomas Haudebourg[1,2], Pauline Peuziat[1,2], Thibault Colombani[1,2], Mathieu Berchel[4], Olivier Lambert[3], Aleksander Edelman[5] and Bruno Pitard[1,2,6]

The intracellular delivery of biologically active protein represents an important emerging strategy for both fundamental and therapeutic applications. Here, we optimized *in vitro* delivery of two functional proteins, the β-galactosidase (β-gal) enzyme and the anti-cytokeratin8 (K8) antibody, using liposome-based formulation. The guanidinium-cholesterol cationic lipid bis (guanidinium)-tren-cholesterol (BGTC) (bis (guanidinium)-tren-cholesterol) combined to the colipid dioleoyl phosphatidylethanolamine (DOPE) (dioleoyl phosphatidylethanolamine) was shown to efficiently deliver the β-gal intracellularly without compromising its activity. The lipid/protein molar ratio, protein amount, and culture medium were demonstrated to be key parameters affecting delivery efficiency. The protein itself is an essential factor requiring selection of the appropriate cationic lipid as illustrated by low K8 binding activity of the anti-K8 antibody using guanidinium-based liposome. Optimization of various lipids led to the identification of the aminoglycoside lipid dioleyl succinyl paromomycin (DOSP) associated with the imidazole-based helper lipid MM27 as a potent delivery system for K8 antibody, achieving delivery in 67% of HeLa cells. Cryo-transmission electron microscopy showed that the structure of supramolecular assemblies BGTC:DOPE/β-gal and DOSP:MM27/K8 were different depending on liposome types and lipid/protein molar ratio. Finally, we observed that K8 treatment with DOSP:MM27/K8 rescues the cyclic adenosine monophosphate (cAMP)-dependent chloride efflux in F508del-CFTR expressing cells, providing a new tool for the study of channelopathies.

Molecular Therapy—Nucleic Acids (2015) **4**, e244; doi:10.1038/mtna.2015.17; published online 23 June 2015
Subject Category: Mechanisms of gene and nucleic acid transfer/transfection Vector trafficking and biodistribution

Introduction

Protein-based therapeutics represents a major breakthrough in medicine with more than 100 proteins approved for clinical use. One recent development has been the use of recombinant proteins, including hormones like the insulin-like growth factor,[1] enzymes[2] and antibodies such as rituximab.[3] All these molecules have extracellular targets which emphasize one of the major current limitations of this therapy namely the lack of an efficient way to deliver functional polypeptides into the cell. Numerous proteins need to be transported intracellularly to exert their therapeutic action but do not spontaneously cross plasma membranes due to their important size and biochemical properties. New methods to deliver functionally active proteins into the cells would extend use of therapeutic proteins to attractive intracellular targets and would be a powerful tool for laboratory investigation. Furthermore, protein delivery could overcome some drawbacks of gene therapy, in particular the difficulty of controlling expression levels and the oncogenic risk associated with transgene integration into the host cell genome. For treatments of cancers, infectious diseases or generation of induced pluripotent stem cell, that require only a transient expression of the transgene, delivery of protein represents a promising and safe approach.

In this context, various strategies are currently available for intracellular delivery. Microinjection allows the efficient transduction of a controlled amount of protein directly into the cell cytoplasm, but can only be applied to a small number of cells. Electroporation also allows the transport of therapeutic molecules. Electric pulse delivery created permeabilized areas in the cell membrane but has associated undesirable characteristics like damaging effects to the membrane affecting viability and poor cell targeting. Recently, new methods involving engineering of the protein to be delivered have been developed. However, this technology requires its fusion with a particular class of peptides named protein transduction domains (PTDs) or cell penetrating peptides (CPPs)[4,5] which can interfere with protein folding, leading to a loss of biological function. Another attractive nonviral gene transfer approach is based on lipid encapsulation. Cationic lipids have shown to be efficient vehicle for transmembrane delivery of nucleic acids such as DNA or siRNAs and have more recently been used to transfer proteins.[6–8] Lipid-based delivery system does not require protein engineering step, the procedure is simplified and the amount of protein required reduced. Over the past few decades, liposomes have evolved from being inert drug carriers to highly responsive delivery system, with active targeting, increased stealth, and controlled drug-release properties.[9] These amphiphilic compounds spontaneously associate with oligonucleotides forming supramolecular assemblies taken up by cells. The mechanism of action is well established, having been studied extensively for gene transfer process.[10] The positively charged macromolecule/lipid complex interacts with the negatively charged cell plasma membrane, leading to its internalization through endocytosis. Once in the

[1]Unité INSERM UMR 1087, CNRS UMR 6291, Nantes, France; [2]Université de Nantes, L'institut du Thorax, Nantes, France; [3]CBMN UMR-CNRS 5248, Université de Bordeaux IPB, Pessac, France; [4]UMR CNRS 6521, IFR 148 ScInBioS, Université de Bretagne Occidentale, Université Européenne de Bretagne, Brest, France; [5]Faculté de médecine Paris-Descartes, INSERM U845, Paris, France; [6]Present address: InCellArt, Nantes, France. Correspondence: Bruno Pitard, InCellArt 21 rue La Noue-Bras-de-Fer 44200 Nantes – France. E-mail: bruno.pitard@univ-nantes.fr
Keywords: antibody delivery; ionizable lipids; intracellular delivery; supramolecular assembly
Received 13 November 2014; accepted 17 April 2015; published online 23 June 2015. doi:10.1038/mtna.2015.17

endocytic pathway, the cargo molecule avoids lysosomal degradation and reaches cytosol by destabilization of the endosomal membrane structure.[11] The ability of liposomes to cross plasma membranes and deliver their cargoes into the cytoplasm greatly depends on their physico-chemical properties. Although the properties of lipoplexes are well known,[12] protein-based complexes are still ill defined. Thus, there is a need to develop and characterize efficient and safe synthetic intracellular protein delivery systems.

In the present study, we have identified cationic lipid formulations able to deliver into cells two types of proteins, enzyme and antibody. The guanidinium-cholesterol cationic lipid bis (guanidinium)-tren-cholesterol (BGTC) was combined to the colipid dioleoyl phosphatidylethanolamine (DOPE) to efficiently transport the β-galactosidase (β-gal) enzyme intracellularly. Transfection parameters (lipid/protein molar ratio, cytotoxicity, and culture medium) were optimized and β-gal activity quantified confirming that protein structure and function were not modified as a result of complexation. The aminoglycoside lipid dioleyl succinyl paromomycin (DOSP) associated with the imidazole-based helper lipid MM27 was shown to achieve intracellular delivery of biologically active anti-cytokeratin 8 (K8) antibody. The relationship between the physicochemical properties of these two supramolecular assemblies and their transfection efficiency were investigated by cryo-transmission electron microscopy (cryo-TEM). Finally, we evaluated the liposome DOSP:MM27 as a potential delivery system of the K8 therapeutic antibody for cystic fibrosis (CF). CF is a frequent and lethal disease, caused by mutation in the gene encoding the chloride channel cystic fibrosis transmembrane conductance regulator (CFTR). More than 1,900 mutations of the *CFTR* gene have been described, although the deletion of the phenylalanine residue at position 508 (F508del) is the most abundant in CF patients, with an occurrence of approximately 70%. F508del causes retention of the mutated-CFTR in the endoplasmic reticulum preventing the correct localization of CFTR channels at the plasma membrane.[13,14] It was shown that K8 protein interacts with F508del-CFTR and is implicated in its retention in endoplasmic reticulum.[15] Thus, we tested whether delivering K8 antibody to F508del-CFTR expressing HeLa cells would destabilize F508del-CFTR and K8 interaction leading to the functional plasma membrane expression of F508del-CFTR.

Results

Optimization of the lipid/protein formulation for β-galactosidase delivery

Based on the screening of a cationic lipid library, we identified two compounds able to deliver β-galactosidase (β-gal) in cultured HeLa cells. **Figure 1a** shows that the fatty acid derivative DOSP, and the cholesterol derivative BGTC, complexed with β-gal at various cationic lipid/protein molecular ratios (MR),

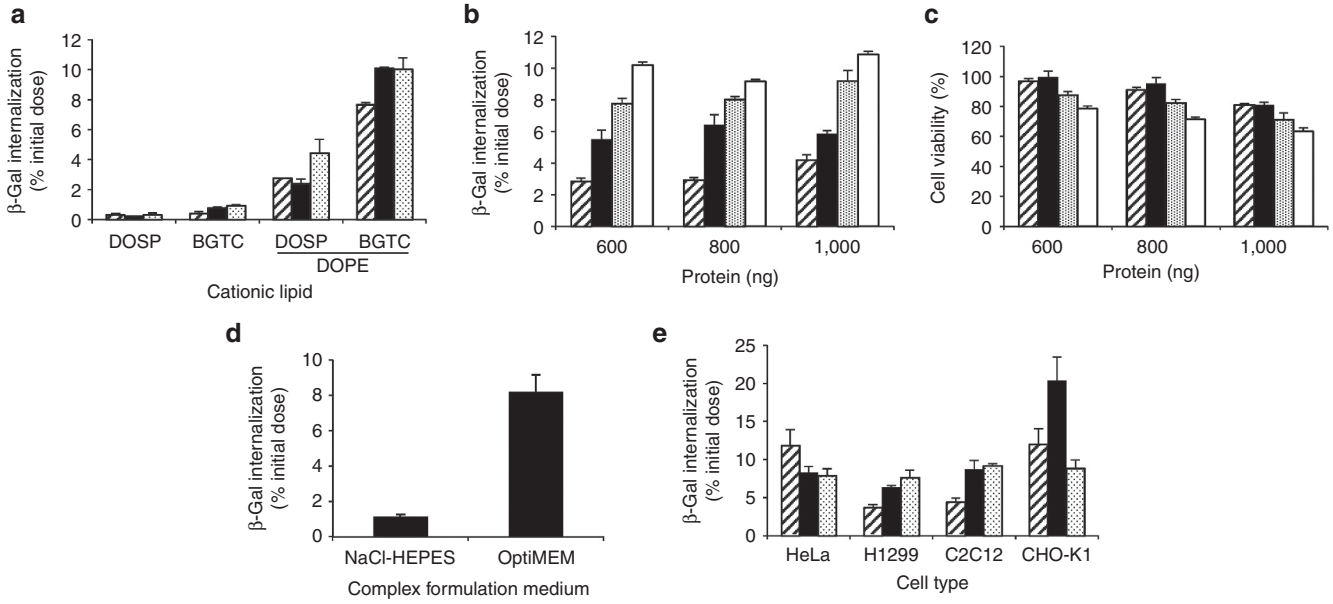


Figure 1 Intracellular delivery of the reporter protein β-gal complexed with various lipid formulations. (**a**) Internalization of β-gal complexed with micelles composed of bis (guanidinium)-tren-cholesterol (BGTC) or DOSP and liposomes formed of BGTC:DOPE or DOSP:DOPE in HeLa cells. β-gal protein (800 ng) was formulated with cationic lipids in OptiMEM at various lipid/protein molar ratio (MR): 1000 (dashed bars), 1,500 (black bars), or 2,000 (dotted bars). Complexes were added on cells for 8 hours before cells lysis and β-gal activity measurement. Results are expressed as percentage of the initial dose of protein used to form complexes. (**b,c**) Effect of protein amount and MR on internalization efficiency and cytoxicity in HeLa cells. β-gal protein (600, 800, 1,000 ng) was formulated with BGTC:DOPE in OptiMEM at various MR: 1,000 (dashed bars), 1,500 (black bars), 2,000 (dotted bars), or 2,500 (white bars). Percentage of internalization and cell viability were assessed by β-gal activity measurement and MTT assay respectively. (**d**) Effect of the formulation medium on transfection efficiencies. Percentage of β-gal internalization was evaluated by delivering 800 ng of protein formulated with BGTC:DOPE at a MR of 2,000 in NaCl-HEPES or OptiMEM medium. (**e**) Internalization of β-gal complexed with BGTC:DOPE in various cell types. β-gal protein (800 ng) was formulated with liposomes in OptiMEM at various lipid/protein molar ratio (MR): 1,000 (dashed bars), 1,500 (black bars), or 2,000 (dotted bars) and incubated with HeLa, H1299, C2C12, or CHO-K1 cells. Results are expressed as the mean percentage of three representative experiments ± SD.

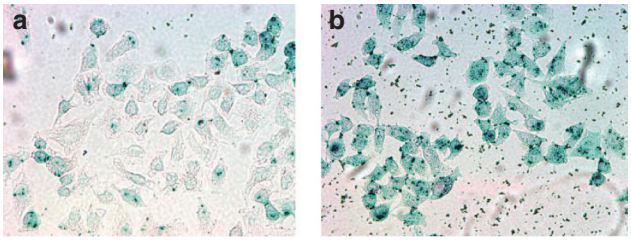


Figure 2 β-gal internalization over time in HeLa cells. β-gal protein (800 ng) was complexed with bis (guanidinium)-tren-cholesterol (BGTC):DOPE at a MR of 1,500. Complexes were added onto cells in serum-free DMEM for 15 minutes (**a**) or 4 hours (**b**). Cells were subsequently washed, fixed and stained with X-gal.

led to β-gal internalization into cells. These cationic lipids used alone as micelles showed a limited efficacy, but combined with the neutral lipid DOPE to form liposomes, dramatically increased the internalization efficiency (0.3 ± 0.1% for DOSP versus 4.44 ± 0.8% for DOSP:DOPE and 0.94 ± 0.05% for BGTC versus 10.1 ± 0.6% for BGTC:DOPE of β-gal intracellular delivery, MR 2,000). Spontaneous internalization of β-gal was not seen in these conditions. We further optimized the efficiency of the delivery by exploring the properties of the BGTC:DOPE formulation. The effect of increased amount of protein on internalization efficiency was assessed in parallel with cytotoxic effect. **Figure 1b** shows that the percentage of protein internalized into cells increased with the lipid/protein MR reaching ~10% of the protein initial dose, whereas no significant increase was achieved using growing amount of β-gal (600–1,000 ng) at a fixed MR. We observed that the optimal protein delivery was achieved with 1,000 ng of β-gal complexed with BGTC:DOPE using a MR of 2,500, which led to a 40% reduction in cell viability (**Figure 1c**). To avoid extensive cell death, we chose to work with 800 ng of protein complexed with BGTC:DOPE at a MR of 1,500 leading to the delivery of 6% of the protein into the cells without compromising their viability. We next investigated the impact of the formulation medium of BGTC:DOPE/β-gal complexes on protein delivery process. The amount of internalized β-gal showed a sevenfold increase in uptake of complexes formulated in OptiMEM compared to NaCl-HEPES buffer (8.2 ± 1.2% for OptiMEM versus 1.14 ± 0.2% for NaCl-HEPES of β-gal internalization, **Figure 1d**). Finally, the ability of BGTC:DOPE to deliver proteins into various cell lines was assessed. **Figure 1e** shows that BGTC:DOPE triggered β-gal internalization in lung carcinoma cells (H1299) myoblasts (C2C12) and ovary cells (CHO-K1), with similar effectiveness than in HeLa cells.

To investigate the localization of β-gal after intracellular internalization and validate that internalized protein is functional, HeLa cells were incubated with BGTC:DOPE/β-gal complexes and an X-gal staining was performed on cells after 15 minutes or 4 hours. Results showed that for short incubation time (15 minutes), the β-gal activity was low as illustrated by the faint blue color in cell cytosol (**Figure 2a**). In contrast, after 4 hours, the cells exhibited a dense blue color within the cytoplasm highlighting an enhanced β-gal activity corresponding to an increase of functional enzyme within the cytoplasm after probably its release from endosome (**Figure 2b**)

Optimization of the lipid/protein formulation for K8 antibody delivery

In recent years, therapeutic antibodies have been shown to be of great importance for clinical use. Expanding their application to intracellular targets is an emerging concept that would have many applications mainly by modulating intracellular protein-protein interactions. With this aim, we tested the ability of cationic lipids to deliver an antibody in its native conformation, thus capable of recognizing its antigenic intracellular target. An fluorescein isothiocyanate (FITC)-tagged monoclonal immunoglobulin directed against human cytokeratin 8 (FITC-K8) was delivered into HeLa cells using BGTC and DOSP associated or not with the colipid DOPE (**Figure 3a**,**b**,**d**,**e**). After 4 hours of incubation, only few cells displayed cytoplasmic fluorescence and K8 antibody was mostly detected in complexes surrounding the cells. This prompted us to test whether a different neutral colipid could improve the antibodies delivery. The formulation of BGTC as liposomes with the imidazole-based helper lipid named MM27, did not lead to a significant change in the percentage of positive cells (**Figure 3c**). However, the use of the DOSP:MM27 formulation dramatically increased the number of FITC-labeled cells (**Figure 3f**,**g**,**h**). The percentage of K8-labeled cells was quantified and revealed that 67% of the total population was transfected using the DOSP:MM27 formulation compared to 14 and 8% with DOSP:DOPE and BGTC:MM27 respectively (**Figure 3i**).

DOSP:MM27-mediated anti-K8 antibody delivery led to an intense labeling of the cell cytoskeleton, visible after 4 and 24 hours (**Figure 4a**,**b**) of incubation with the complexes, demonstrating the ability of DOSP:MM27 liposomes to deliver the antibody over an extended period of time. Although fixation can produce artifacts, the cytoskeletal staining pattern observed in PFA-fixed HeLa cells treated with DOSP:MM27/FITC-K8 liposomes (**Figure 4c**) was comparable with the staining seen in living cells after transfection (**Figure 4a**,**b**). In order to confirm the capacity of the liposome to achieve intracellular delivery of biologically active FITC-K8 antibody, cells transfected with DOSP:MM27/FITC-K8 were fixed, permeabilized, and then incubated with a rabbit polyclonal anti-K8 antibody, followed by immunostaining with a secondary anti-rabbit AlexaFluor 546. FITC-K8 and K8 antibodies recognize different epitopes on the same K8 target, respectively the C-terminus and the N-terminus around the serine at position 73. Confocal microscopy observation (**Figure 4d**) revealed that FITC-K8 delivered by liposome localized mainly on fiber structures characteristic of cytoskeletal staining pattern. In addition, FITC-K8 appeared to colocalize with the AlexaFluor 546 signal resulting from K8 immunostaining providing evidence of the functionality of the delivered antibody (**Figure 4e**,**f**).

Physicochemical characterization of BGTC:DOPE/β-gal and DOSP:MM27/K8 complexes

Next, we investigated the physicochemical properties of the complexes obtained by mixing β-gal or K8 antibody with BGTC:DOPE or DOSP:MM27 liposomes respectively. Migration of BGTC:DOPE/β-gal assemblies was performed on a native polyacrylamide gel electrophoresis to precisely quantify protein complexation by the cationic molecules.

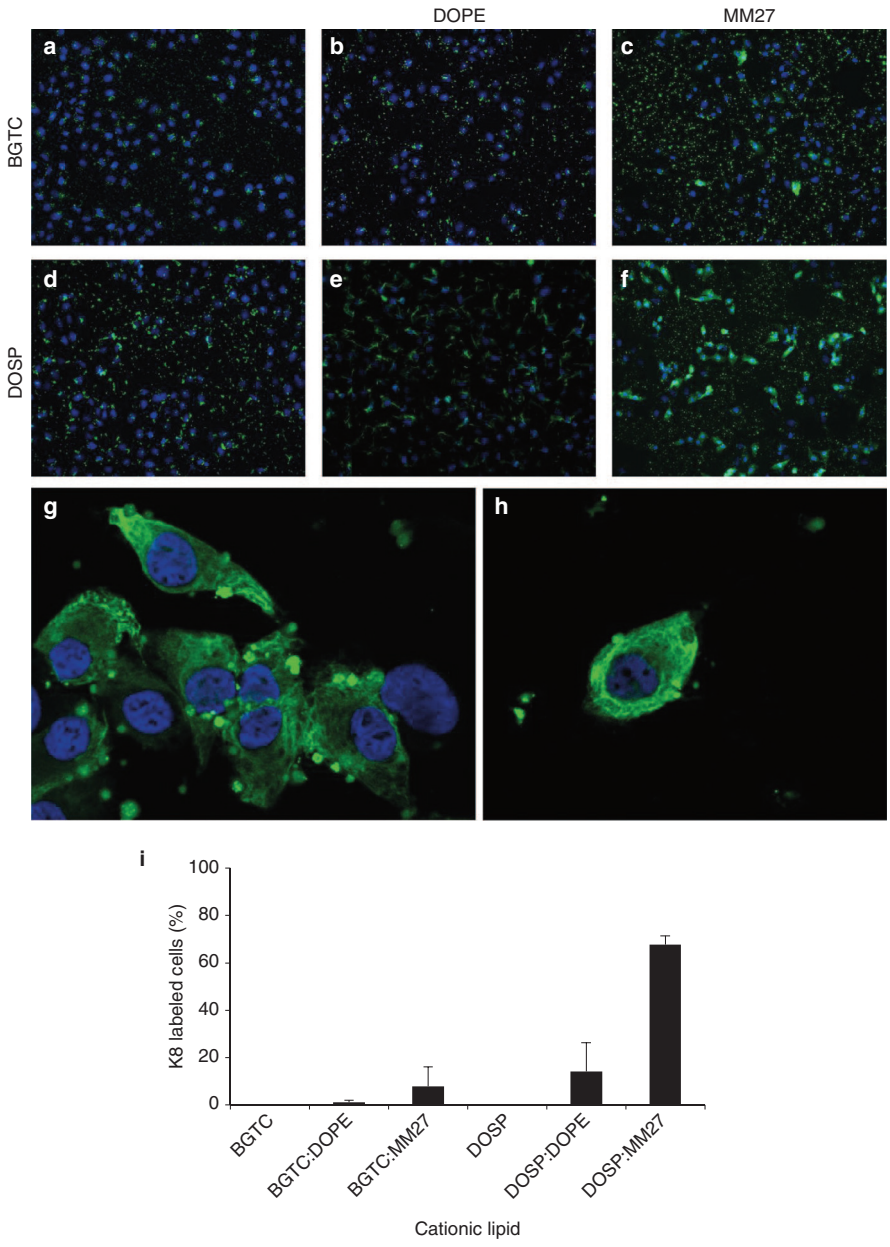


Figure 3 Intracellular delivery of the FITC-K8 antibody complexed with various lipid formulations. Hela cells were treated with FITC-K8 (800 ng) formulated with bis (guanidinium)-tren-cholesterol (BGTC) (**a**), BGTC:DOPE (**b**), BGTC:MM27 (**c**), DOSP (**d**), DOSP:DOPE (**e**), or DOSP:MM27 (**f**) (**g**) and (**h**), at a molar ratio of 1,500. In each condition, cells were incubated for 4 hours with the lipid/FITC-K8 complexes before fixation and mounting with ProLong antifade DAPI reagent. (**i**) Quantification of K8-positive cells after transfection with BGTC, BGTC:DOPE, BGTC:MM27, DOSP, DOSP:DOPE, and DOSP:MM27. Results are expressed as the mean percentage of three representative experiments ± SD.

Figure 5a shows that the amount of uncomplexed β-gal, free protein migrating through the gel, decreased rapidly as the MR raised with a consequent amount of β-gal complexed with BGTC:DOPE at a molar ratio of 100. Lipid/protein MR above 200 resulted in aggregates that did not migrate out of the well showing that BGTC:DOPE liposome allowed the efficient complexation of the protein and its compaction into stable complexes at high MR. Protein complexation was also evaluated for FITC-K8 antibody and DOSP:MM27. Fluorescent analysis was used to determine the amount of residual free antibody present in supernatant after DOSP:MM27/FITC-K8 formulation depending on lipid/protein MR. Figure 5b shows that around 40% of FITC-K8 was associated with DOSP:MM27 at a MR of 100. Elevating the MR increased the percentage of FITC-K8 complexation with 100% FITC-K8 associated with DOSP:MM27 from a MR of 400.

To further elucidate the mechanism of action of liposomes, various lipid mixture conditions were analyzed by cryoTEM. Figure 6 shows the morphology and assembly of the supramolecular complexes of BGTC:DOPE/β-gal using different MR. At high MR of 1,500, liposomes were generally spherical unilamellar vesicles forming large aggregates (Figure 6a–c).

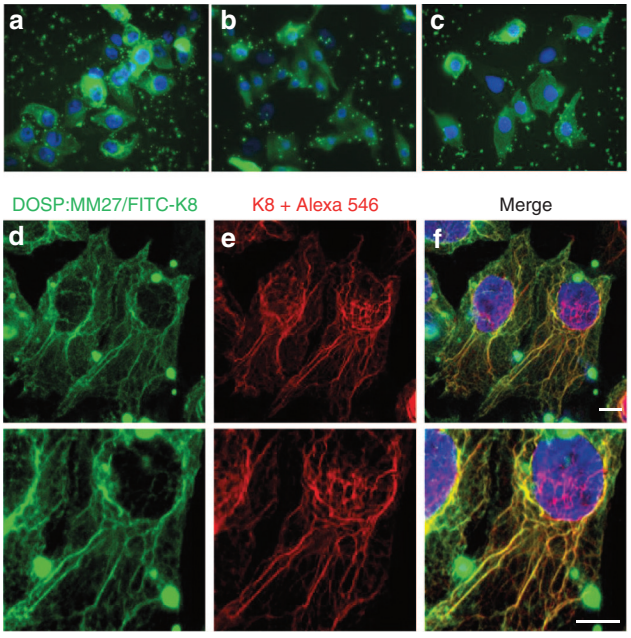


Figure 4 Intracellular localization of FITC-K8 antibody delivered by DOSP:MM27 liposome. Hela cells were plated on 24-well plate and incubated with DOSP:MM27/FITC-K8 complexes for 4 hours (**a**) or 24 hours (**b**) and observed under microscope without further treatment. Hela cells were plated on 24-well plate, incubated with DOSP:MM27/FITC-K8 complexes for 4 hours and fixed with PFA before microscope observation (**c**). Hela cells were plated on glass coverslips, incubated with DOSP:MM27/FITC-K8 complexes for 4 hours, fixed and immunostained with a rabbit anti-K8 and a secondary anti-rabbit AlexaFluor® 546 (red). Nuclei stained using DAPI (blue), FITC-K8 (green) (**d**) and K8 staining (red) (**e**) are visualized under confocal fluorescence microscope as superimposition of images (merge) (**f**). Lower panel shows higher magnification. Scale bar = 10 µm.

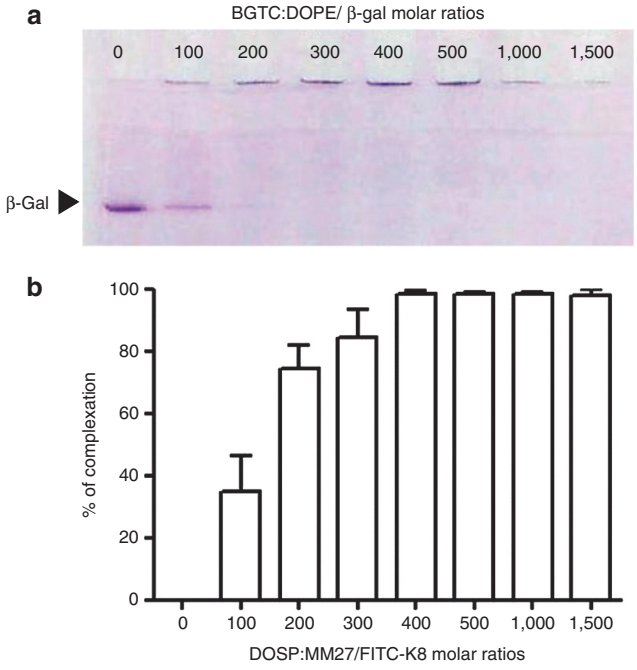


Figure 5 Complexation of the β-gal anti-FITC-K8 protein with the BGTC:DOPE or DOSP:MM27 lipids depending on molar ratios. Lipid-proteins complexes were formed in OptiMEM at various molar ratios (100–1,500) and nonassociated proteins were visualized on a native-PAGE gel for the β-gal (**a**) or measured by fluorospectrometer for the FITC-K8 (**b**).

The β-gal protein appeared to be entrapped within aggregates, occasionally forming protein layers/junctions between two lipid membranes (black arrows). At a MR of 750 (**Figure 6d–f**), protein junctions were more frequently encountered suggesting a higher amount of protein bound to liposome surfaces. The particles displayed more polymorphic structures: spherical vesicles coexist with vesicles of irregular shape as well as multiwalled and fused vesicles. At a MR of 375 (**Figure 6g–i**), liposomes formed larger isolated multilamellar objects decorated with proteins on their external surfaces (white arrows).

In order to explain the significant difference in the K8 delivery efficiency between formulations, we next investigated by cryoTEM the structure of complexes formed with K8 and various liposome preparations. BGTC:DOPE and BGTC:MM27 lipid mixtures formed unilamellar liposomes. In the presence of K8 antibody, both mixtures formed micron-size aggregates due to protein–lipid interaction (**Figure 7a,b**). For BGTC:DOPE, protein densities were visible at liposome surface as well as between lipid membranes without forming regular organization (white arrows, **Figure 7a**). DOSP:DOPE mixture produced liposomes, heterogeneous in size and lamellar organization. In contact with anti-K8, liposome aggregation was observed, indicative of a strong protein–lipid interaction (**Figure 7c**). However, it remained difficult to provide structural details on lipid/protein interaction due to liposome heterogeneity. Unlike others, DOSP:MM27 mixture was not organized in liposome but in 20 nm domains showing no evidence of internal structure. When mixed with anti-K8 antibody, DOSP:MM27 formed 1–2 µm lipoplexes consisting of aggregated spherical elements (**Figure 7d**). At higher magnification, these spherical arrangements were seen as "onion-like" concentric multilamellar structures of 100–200 nm diameter exposing protein densities at their surfaces (white arrows **Figure 7d**) but internally devoid of proteins.

Functional impact of anti-K8 antibody delivery on F580del-CFTR trafficking

We finally tested the ability of the DOSP:MM27/K8 complexes to restore the F508del-CFTR trafficking in mutated HeLa cells. It was demonstrated that K8 was bound directly to the F508del *in vivo* causing retention of the mutated F508del-CFTR channel in the endoplasmic reticulum and its absence in the plasma membrane.[16] Furthermore, it was shown that inhibition of K8 expression by pharmacological molecules or siRNA in F508del-expressing HeLa cells led to the recovery of CFTR-dependent iodide efflux.[15,16] On the basis of this recent discovery, we hypothesized that delivering K8 antibody to F508del-CFTR expressing HeLa cells would disrupt F508del-CFTR and K8 interaction leading to the correction of the F508del-CFTR trafficking defect. It is known that the interaction between F508del-CFTR and K8 occurs through the N-terminal of the K8 protein. In order to ensure that the observed effect is specific, we used an antiK8 recognizing the C-terminus of the K8 target as an irrelevant antibody control.

The recovery of F508del-CFTR processing was monitored by measuring the cAMP-dependent anionic conductance

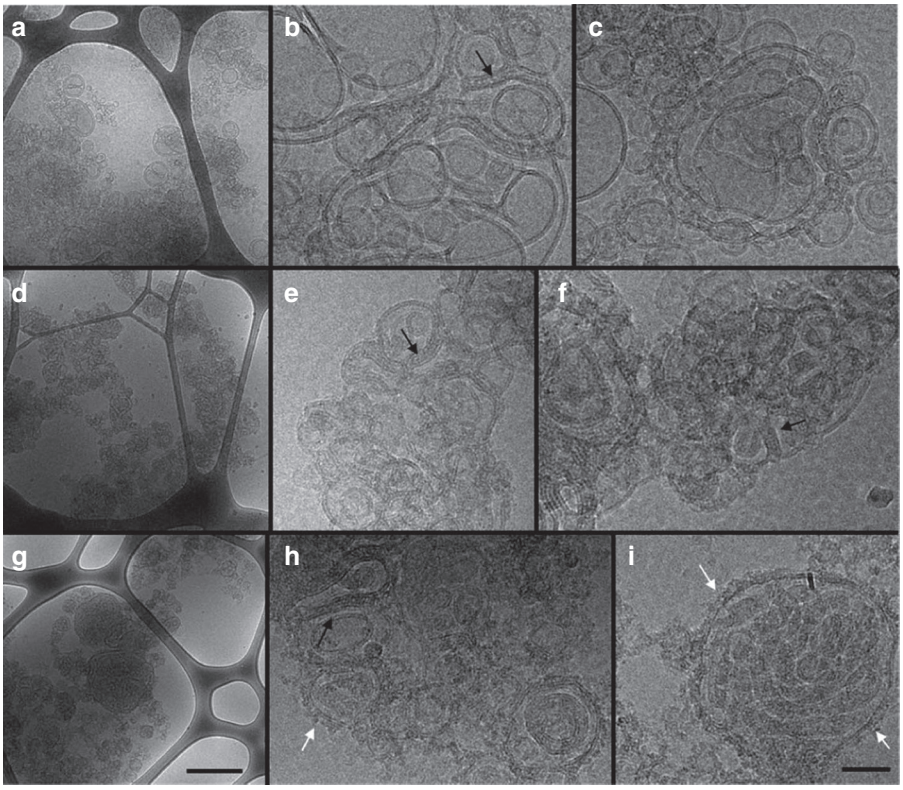


Figure 6 CryoTEM images of β-gal complexed with BGTC:DOPE liposomes formulated at various cationic lipid/protein ratios. (**a–c**) MR = 1,500; (**d–f**) MR = 750; (**g–i**) MR = 375. Black arrows denote β-gal protein accumulation forming junctions between lipid membranes. White arrows denote protein densities coated at the surface of liposomes. Scale bars, 0.5 µm (**a,d,g**) and 50 nm (**b,c,e,f,h,i**).

through the plasma membrane of F508del-CFTR expressing cells using halide-sensitive probe, 6-methoxy-N-ethylquinolinium iodide (MEQ) (**Figure 8**). Upon addition of cAMP to initiate channel opening and exchange of extracellular I^- for nitrate $NO3^-$, MEQ fluorescence increased in WT-CFTR expressing cells (triangles) as CFTR-mediated anion transport results in replacement of intracellular I^- with nonquenching NO_3^-. Under iodide perfusion, fluorescence of intracellular MEQ was rapidly quenched by entry and collision with iodide ions. WT-CFTR expressing cells treated or not with DOSP:MM27/K8 displayed a similar behavior but a reduced fluorescence amplitude was detected in nontreated cells. In contrast, F508del-CFTR expressing cells, untreated (cross) or treated with DOSP:MM27/antiK8 C-ter (circle), showed a weak response with a low anionic conductance illustrated by the attenuated fluorescence changes. Finally, F508del-CFTR expressing cells transfected with DOSP:MM27/antiK8 N-ter (diamonds) displayed a robust and prompt increase in MEQ fluorescence under cAMP stimulation, followed by a rapid quenching after iodide perfusion. Altogether, these results indicate that delivering K8 antibody into F508del-CFTR expressing cells using liposomes rescues cAMP-dependent anionic conductance, suggesting a partial restoration of F508del-CFTR channel trafficking towards the plasma membrane.

Discussion

In this study, we demonstrate rapid and efficient delivery of catalytic protein and antibodies into the cytosol of cultures cells using liposome-based formulation. Intracellular delivery of functional proteins provides a potential tool to replace missing, dysfunctional and poorly expressed proteins or antagonize key intracellular pathways. Protein-based therapeutics is a promising approach for several biomedical applications including stem cell engineering, imaging, and signaling studies.

Delivery of β-gal was chosen as a test of the efficacy of lipid formulations since this multimeric enzyme is susceptible to inactivation during the delivery process. The availability of a highly sensitive detection test, and the possibility to observe its presence in the cell cytoplasm by X-gal staining, allowed us to perform a screening of cationic lipids library. Furthermore, as detection is based on enzymatic activity, this is a stringent way to ascertain that analyzed compounds deliver proteins that retain, at least partially, their active conformation. Although most of the cationic lipids tested proved to be inefficient to deliver the enzyme into cultured HeLa cells, two molecules, DOSP and BGTC, were able to transport a low but detectable amount of the initial protein dose into the cells when used as micellar solutions. BGTC is a cholesterol-based lipid bearing two guanidinium polar head-groups[17] and DOSP is a fatty-acid-based molecule bearing a paromomycin head-group.[18,19] These two compounds are commonly used for their high DNA and siRNA transfection potentials and their lack of toxicity. In order to enhance their protein delivery activities, we formulated them as liposomal suspensions combined with the neutral lipid, DOPE. We observed a dramatic increase in the activity for DOSP:DOPE and BGTC:DOPE without noticeable toxicity. DOPE is commonly

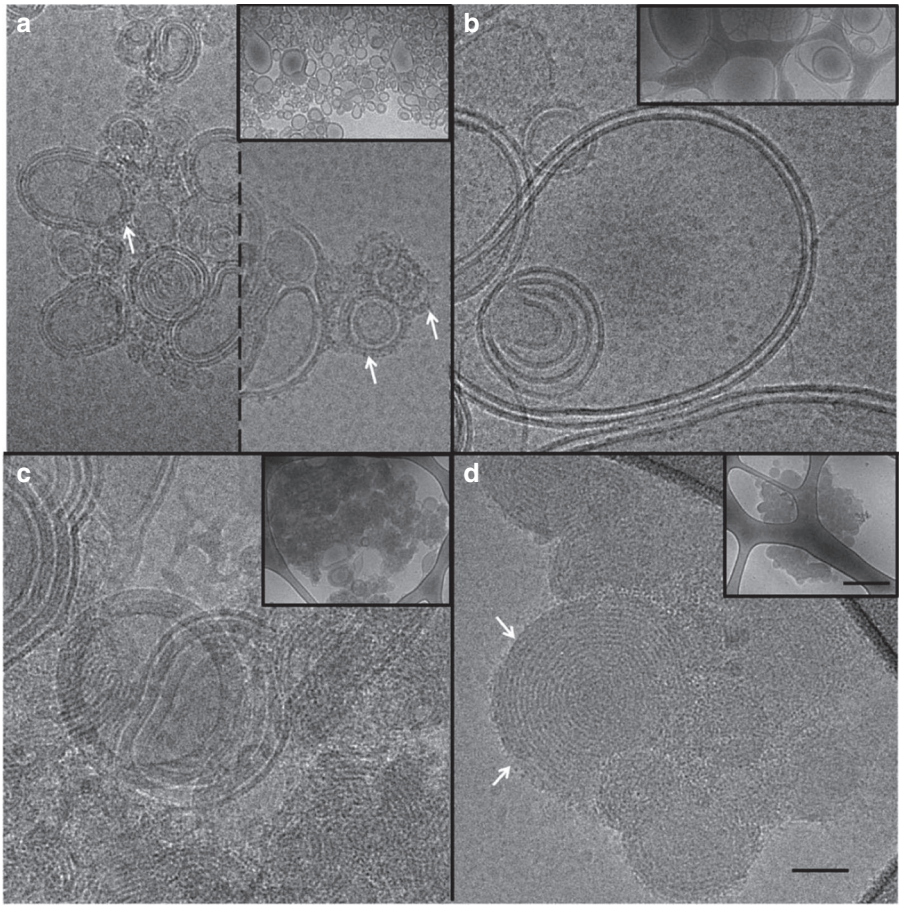


Figure 7 CryoTEM images of cationic lipid/K8 antibody complexes. (**a**) BGTC:DOPE, (**b**) BGTC:MM27, (**c**) DOSP:DOPE, (**d**) DOSP:MM27. White arrows denote protein densities visible at liposome surfaces and between lipid membranes. Insets correspond to a larger view of each condition. Scale bars 50 nm (inset 500 nm).

used in nucleic acid transfection reagents to promote endosomal membrane disruption.[12,20] It is likely that cationic lipids used alone led to the cellular internalization of the protein, followed by lysosomal degradation. Adding DOPE to the formulation would promote the delivery of the enzyme to the cytosol before fusion of endosomes with lysosomes. It is to be noted that cells were lyzed with reporter lysis buffer directly into culture plates following transfection. We assume that the amount of internalized β-gal may be slightly overestimated by quantifying external liposomes that bind cell membrane. Nevertheless, extensive phosphate-buffered saline (PBS) washing removed most of the complexes and microscopy analysis confirmed the delivery of the β-gal into the cytosol. X-gal staining of cells treated with BGTC:DOPE/β-gal lipoplexes showed detectable staining throughout the cytosol of all treated cells, confirming catalytic activity of the enzyme. Interestingly, β-gal activity was still detectable after 24 hours of incubation, indicating a prolonged release of the enzyme into the cells and/or a prolonged protein half-life in the cytosol.

We then investigated whether liposomes could deliver not only enzymes but proteins with binding activities such functional antibodies into HeLa cells. An FITC-tagged antibody directed against human cytokeratin 8 was formulated with BGTC and DOSP, in the presence or absence of DOPE. None of the conditions tested by varying the protein dose and the molar ratio, enabled entry of the antibody into the cells. Microscopy observation showed confined FITC fluorescence staining area suggesting that lipoplexes were trapped in the endosomal system. Lack of efficiency for cationic lipid-mediated antibody delivery has already been observed in previous studies. It was described that antibodies delivered by Saint-2:DOPE were localized in the cell but formed confined staining area, independent of their targets, probably indicating endosomal sequestration of Saint2:DOPE/antibodies.[8] Addressing this issue, we chose to enhance the endosomal escape step by using MM27, an imidazole-bearing neutral lipid. It has been reported previously that this compound is 100-fold more efficient than DOPE in promoting DNA transfection.[21,22] It was shown that the amines of the imidazole head-group, neutral at physiological pH, undergo protonation in acidic organelles, leading to endosomal membrane disruption by a proton-sponge mechanism.[23] We demonstrated that FITC-K8 delivered by DOSP:MM27 localized mainly on fiber cytokeratin network for at least 24 hours, confirming the functionality of the antibody. Moreover, we observed that 70% of treated cells were labeled after 4 hours, showing a dramatic improvement compared with DOSP and DOSP:DOPE-mediated delivery. Altogether, these findings indicate that the efficiency of the delivery system varies greatly depending on the protein type, and that vectors have to be adapted and optimized according to the cargo. This

contrasts with DNA or RNA delivery which takes advantage of the universal structure of nucleic acids. Indeed, nucleic acids, independently of the nucleotide sequence, present the same structure and electrical charge, unlike peptides and proteins, whose physicochemical parameters vary greatly.

We used cryo-TEM to better understand the supramolecular organization of cationic lipid/protein complexes. We observed that the mixing of BGTC:DOPE liposomes with β-gal at the optimal MR of 1,500 promoted aggregation, resulting in large, globally spherical complexes. Protein molecules were present within the aggregates and occasionally formed protein layers between two lipid membranes, so-called protein junctions. As β-gal molecule is a tetramer, it exposed several binding sites for liposome, promoting contacts between two lipid membranes and causing liposomal aggregation. Whereas liposomes were mostly free of protein at their surface at a MR of 1,500, lower MR complexes formed larger isolated objects decorated with proteins on their external surfaces. We hypothesized that protein coating on liposome surface observed at suboptimal MR, prevented liposome aggregation as well as interaction and fusion of liposome with the endosomal membrane. A tight contact between the lipoplex surface and the endosomal membrane is essential to promote mixing of lipids by "flip-flop" between the two bilayers, resulting in endosomal membrane destabilization and disruption.[10,20,24] As a result, the delivered protein is susceptible to degradation in the lysosome and is unable to access cytosol. Based on these observations, we suggest that the optimal ratio of 1,500 corresponds to a balance between two unfavorable situations. For lower ratios, the protein densities, exposed at the liposome surface, prevent the fusion between endosomal membranes and cationic lipids, while toxicity is induced at higher ratios reducing the delivery efficiency.

The study of the liposome structures formed by cationic lipids with the anti-K8 antibody highlights a different mechanism of delivery. DOSP:MM27/K8 showed a unique organization forming clusters of onion-like structures bearing antibodies on their surfaces but devoid of proteins. Such remodeling of cationic lipid-based assemblies to multilamellar concentric structures has already been described with cationic lipid/nucleic acid complexes.[25] This arrangement suggests that liposomes escape endosome through membrane disruption by a proton-sponge mechanism, while the large amount of MM27 per lipoplex offers a high buffering capacity. During endocytic trafficking, endolysosomes are acidified by the action of an ATPase enzyme that transports protons from the cytosol into the vesicle. It is proposed that MM27 prevents acidification of endocytic vesicles, causing the ATPase to transport more protons to reach acidic pH. The accumulation of protons in the vesicle is balanced by an influx of counter ions which ultimately causes osmotic swelling and rupture of the endosome membrane.[26] Through this mechanism, liposomes can be released into the cytosol without requiring a tight contact between the endosomal membrane and the lipoplexes.

Finally, we took advantage of the DOSP:MM27 delivery system to investigate the ability of anti-cytokeratin 8 antibodies to disrupt the interaction between cytokeratin 8 and F508del-CFTR. This interaction has previously been shown to impair the trafficking of this mutated channel toward the plasma membrane where it is partially functional, leading to cystic fibrosis.[15,16,27] The evaluation of transmembrane anionic efflux by MEQ fluorescence measurement showed that the delivery of antibodies against cytokeratin 8 led to the restoration of a cAMP-dependent anionic conductance at the surface of F508del-CFTR-expressing cells. These preliminary results have to be confirmed but strongly suggest that antibody-mediated disruption of the interaction between cytokeratin 8 and F508del-CFTR can restore the trafficking of this mutated channel towards the plasma membrane. This approach would provide a tool for the study of channelopathies and development of future therapeutic strategies.

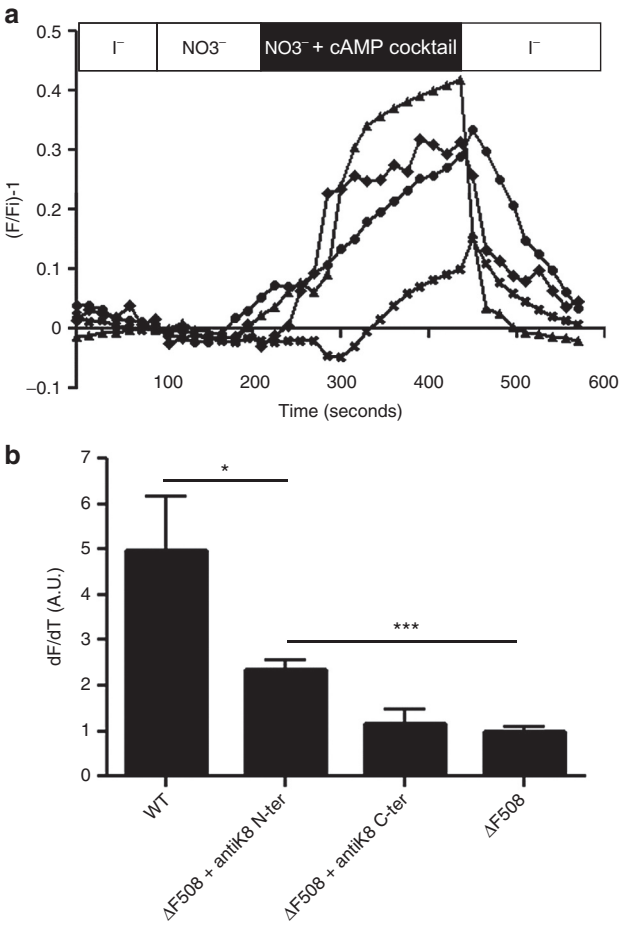


Figure 8 Rescue of F508del-CFTR activity by K8 antibody delivery. (**a**) MEQ fluorescence assay was performed on WT-CFTR cells treated with DOSP:MM27/K8 (triangles), on F508del-CFTR cells treated with DOSP:MM27/antiK8 N-ter (diamonds) or DOSP:MM27/antiK8 C-ter (circle) and untreated F508del-CFTR cells (cross). The fluorescence ratio is calculated as $(F/F_i) - 1$, F = Fluorescence intensity at indicated time points and F_i = Initial fluorescence intensity under iodide perfusion. (**b**) Quenching slopes of MEQ fluorescence registered for 30 seconds upon addition of cAMP and exchange of extracellular nitrate (NO_3^-) for iodide ions (I^-).

Materials and methods

Preparation of liposomes and micelles. The lipids BGTC, DOSP, and MM27 were synthesized respectively as previously described.[18,21] The neutral lipid DOPE (dioleoylphosphatidyl-ethanolamine) was purchased from Avanti Polar Lipids (Alabaster, AL). Liposome formulations were prepared

by dissolving a cationic lipid (BGTC or DOSP) alone or with a neutral lipid (MM27 or DOPE) in chloroform at a molar ratio of 1. The solvent was removed using a rotary evaporator under vacuum at room temperature and the lipidic film rehydrated with ultrapure water for 24 hours at 4 °C at a final concentration of 10 mmol/l. The resulting suspension was sonicated for 15 minutes to obtain liposomes of 100–200 nm diameter.

Formulation of lipid/protein complexes. β-galactosidase (β-gal) (Roche Applied Science, Penzberg, Germany), rabbit anti-cytokeratin 8 antibody (K8) (ab51152, Abcam, Cambridge, UK) or mouse fluorescein conjugated anti-cytokeratin 8 antibody (FITC-K8) (ab87010, Abcam) were diluted with pH 7.4 buffer solution (120 mmol/l NaCl, 20 mmol/l 4-(2-hydroxyethyl)-1-piperazineethanesulfonic acid (HEPES)) or OptiMEM (Life Technologies, Carlsbad, CA) medium to the indicated final concentration. Lipids were diluted in water or OptiMEM at lipid/protein molar ratios (MR) from 100 to 2,500 and added to protein solution (v/v). The resulting solution was mixed gently and incubated for 15 minutes at room temperature before incubation with cells.

Polyacrylamide gel electrophoresis of lipid/protein complexes. BGTC:DOPE/β-gal complexes were prepared with 10 µg β-gal at various lipid/protein MR in pH 7.4 buffer solution (120 mmol/l NaCl, 20 mmol/l HEPES). After 15 minutes incubation at room temperature, 5 µl of the preparation were mixed with 5 µl Blue-Orange loading buffer (Promega, Madison, WI). Migration was performed on a nondenaturing polyacrylamide gel (5% stacking, 7% resolving) for 2 hours and the β-gal protein revealed by Coomassie blue staining.

Spectrofluorometer analysis. DOSP:MM27/anti-K8-FITC antibody complexes were formed in OptiMEM at various molar ratios (100–1,500) and incubated at room temperature for 15 minutes. Samples were centrifuged for 5 minutes at 13,000 g and supernatants were removed for determination of anti-K8-FITC content using a Fluoromax-4 (Horiba scientific, Kyoto, Japan). A standard curve correlating fluorescence and anti-K8-FITC antibody concentration was used to determine the amount of residual free antibody presents in supernatant after complexation.

Cell culture. HeLa (human cervical adenocarcinoma), H1299 (human non-small cell lung carcinoma), and C2C12 (murine myoblasts cells) were cultured in Dulbecco's Modified Eagle's medium (DMEM) (Life Technologies). HeLa cells expressing WT-CFTR or F508del-CFTR were cultured in DMEM supplemented with 450 µg/ml Zeocin (Invivogen, San Diego, CA). CHO-K1 from hamster ovary was cultured in F12-K medium (Life Technologies). All media were supplemented with 2 mmol/l L-glutamine, 10 µg/ml streptomycin, 100 U/ml penicillin, and 10% fetal calf serum obtained from Life Technologies. Cells were cultured at 37 °C in a 5% CO_2 humidified atmosphere.

Protein transfection. The day before transfection, cells were seeded at a density of ~7.0×10^4 cells per well of a 24-well plate in 0.5 ml of the appropriate complete growth medium to obtain 70–80% confluence the day of transfection. For each well, media was replaced 30 minutes before transfection with 0.4 ml of serum-free medium. Lipid/protein complexes prepared in 0.1 ml volume were added to cells. After 4 hours incubation, fetal calf serum was added at a final concentration of 10% and transfection was stopped at indicated time.

β-galactosidase activity assays

β-gal expression quantification. Cells were washed three times with PBS 1× and lysed with 0.3 ml of Reporter Lysis Buffer (Promega) supplemented with a protease inhibitor cocktail (Roche Applied Science). One freeze-thaw cycle was performed to ensure complete lysis. β-gal expression was quantified using the β-Glo Assay system from Promega according to manufacturer instructions. The amount of β-gal originally used for complexation (600, 800, or 1,000 ng) was used as control and arbitrarily fixed at 100%. Luminescence was read using the Victor-X3 multilabel plate reader (Perkin-Elmer, Waltham, MA).

Staining of β-gal-containing cells. HeLa cells were grown on glass coverslips. After treatment, cultures were washed three times with PBS 1×, fixed with 3.7% paraformaldehyde at room temperature and incubated in staining solution (400 µg/ml X-gal, 2 mmol/l $MgCl_2$, 4 mmol/l $K_3[Fe(CN)_6]$, 4 mmol/l $K_4[Fe(CN)_6]$). Slides were mounted with PBS in the presence of glycerol (50% v/v) and observed under an optical microscope.

MTT assay. After treatments, cells were washed, medium was replaced by 100 µl 3-(4,5-dimethylthiazol-2-yl) 2,5-diphenyltetrazodium (MTT) per well (1 mg/ml) diluted in complete medium, and cells were incubated at 37 °C for 4 hours. Then MTT solution was replaced by dimethyl sulfoxide (DMSO) (100 µl/well) and optical density was recorded at 550 nm. All assays were performed in triplicate.

Fluorescence microscopy. The internalization and intracellular fate of the FITC-K8 antibody was visualized 4 and 24 hours following lipid transfection. Cells were washed with PBS and fixed with 3.7% paraformaldehyde solution for 10 minutes at room temperature. Glass coverslips were mounted with ProLong antifade DAPI reagent (Life Technologies) and visualized with a Zeiss (Oberkochen, Germany) Axiovert epifluorescence microscope.

In order to confirm the association of the FITC-K8 antibody with its K8 target, cells were first transfected with the mouse FITC-K8 using DOSP:MM27 liposome, fixed and subsequently stained with the rabbit anti-K8 and a secondary anti-rabbit AlexaFluor 546. In brief, cells were fixed in PBS containing 3.7% paraformaldehyde and permeabilized with PBS containing 4% bovine serum albumin (BSA) (Sigma) and 0.1% saponin (Sigma, Saint-Louis, MO) for 20 minutes. Cells were washed with PBS, blocked with 10% goat serum diluted in PBS-4% BSA-0.1% saponin for 1 hour. Coverslips were then incubated with anti-K8 (1:200 dilution) antibodies overnight at 4 °C. Cells were rewashed and incubated for 1 hour with goat anti-rabbit AlexaFluor 546 (1:2,000 dilution) (Life Technologies) and mounted with ProLong antifade DAPI reagent. Colocalization was visualized using a laser-scanning confocal microscope (Carl Zeiss). Images were treated using ImageJ 1.42q software.

Cryo-TEM. Cryo-TEM imaging of cationic lipid/protein complexes were performed as previously described.[28] Complexes were formulated in 120 mmol/l NaCl and 20 mmol/l HEPES,

pH 7.4, and a 5 µl sample drop was applied to a holey carbon coated copper grid, the excess was blotted with a filter paper, and the grid was plunged into a liquid ethane bath cooled with liquid nitrogen (Leica EM CPC). Specimens were observed at a temperature of ~–170 °C, using a cryo holder, with a FEI Tecnai F20 electron microscope operating at 200 kV. Images were recorded with a 2k × 2k SlowScan CCD camera (Gatan) at a nominal magnification of 50,000× under low-dose conditions.

MEQ fluorescence assay. HeLa cells stably expressing WT-CFTR or F508del-CFTR were grown on glass coverslips for 24 hours and K8 antibody was delivered using DOSP:MM27 in serum-free medium (RM1500, 1.5 µg antibody). Four hours after antibody treatment, MEQ probe was loaded into cells by hypotonic shock permeabilization. Cells were washed with an iodide-containing isotonic solution (138 mmol/l NaI, 2.4 mmol/l K_2HPO_4, 0.8 mmol/l KH_2PO_4, 10 mmol/l HEPES, 1 mmol/l $CaSO_4$, 10 mmol/l D-glucose, pH 7.4) and incubated for 2 minutes in a hypotonic solution containing the halide-sensitive probe, MEQ (Life Technologies) (10 mmol/l MEQ, 110 mmol/l NaI, 1.92 mmol/l K_2HPO_4, 0.64 mmol/l KH_2PO_4, 8 mmol/l HEPES, 0.8 mmol/l $CaSO_4$, 8 mmol/l D-Glucose, pH 7.4). Hypotonic solution was removed and cells incubated with the isotonic solution for 15 minutes recovery. Coverslips were mounted in perfusion chamber continuously supplied with the isotonic solution at 37 °C, and basal fluorescence level observed under a Leica DMI6000B epifluorescence microscope equipped with environmental control. Cells were subsequently perfused with a nitrate-containing solution (138 mmol/l $NaNO_3$, 2.4 mmol/l K_2HPO_4, 0.8 mmol/l KH_2PO_4, 10 mmol/l HEPES, 1 mmol/l $CaSO_4$, 10 mmol/l D-Glucose, pH 7.4) and a cAMP stimulatory cocktail (500 µmol/l cptAMPc, 25 µmol/l forskolin, 100 µmol/l IBMX) was added to initiate channel opening. After 180 seconds, nitrate-containing solution was finally replaced by iodide isotonic solution to quench MEQ fluorescence. Intracellular fluorescence was monitored over time using MetaFluor software (Molecular Devices, Sunnyvale, CA). Results are expressed as relative fluorescence (F/F_i) - 1, F is the fluorescence intensity at time points indicated on the x-axis after background subtraction and compensation of MEQ photobleaching, and F_i the basal MEQ fluorescence obtained under iodide perfusion.

Acknowledgments. The authors are very grateful to the Cellular and Tissular Imaging Core Facility of Nantes University (MicroPICell) for excellent technical expertise in cell imaging. They are also indebted to Pierre and Jean-Marie Lehn for their pioneer works related to the synthesis of cationic lipids used in this study and also to Paul-Alain Jaffres for his work on imidazole based-lipids. This work was supported by special grants from the "Association Française contre les Myopathies" (Evry, France), from "Agence Nationale de la Recherche" (Paris, France) for IHU-CESTI, and from BPIFrance financement (Paris, France) for Emerit and Hepavac.

1. Fintini, D, Brufani, C and Cappa, M (2009). Profile of mecasermin for the long-term treatment of growth failure in children and adolescents with severe primary IGF-1 deficiency. *Ther Clin Risk Manag* **5**: 553–559.
2. Aviezer, D, Brill-Almon, E, Shaaltiel, Y, Hashmueli, S, Bartfeld, D, Mizrachi, S *et al.* (2009). A plant-derived recombinant human glucocerebrosidase enzyme–a preclinical and phase I investigation. *PLoS One* **4**: e4792.
3. Maloney, DG (2012). Anti-CD20 antibody therapy for B-cell lymphomas. *N Engl J Med* **366**: 2008–2016.
4. Ho, A, Schwarze, SR, Mermelstein, SJ, Waksman, G and Dowdy, SF (2001). Synthetic protein transduction domains: enhanced transduction potential *in vitro* and in vivo. *Cancer Res* **61**: 474–477.
5. Järver, P and Langel, U (2006). Cell-penetrating peptides–a brief introduction. *Biochim Biophys Acta* **1758**: 260–263.
6. Zelphati, O, Wang, Y, Kitada, S, Reed, JC, Felgner, PL and Corbeil, J (2001). Intracellular delivery of proteins with a new lipid-mediated delivery system. *J Biol Chem* **276**: 35103–35110.
7. Dalkara, D, Zuber, G and Behr, JP (2004). Intracytoplasmic delivery of anionic proteins. *Mol Ther* **9**: 964–969.
8. van der Gun, BT, Monami, A, Laarmann, S, Raskó, T, Slaska-Kiss, K, Weinhold, E *et al.* (2007). Serum insensitive, intranuclear protein delivery by the multipurpose cationic lipid SAINT-2. *J Control Release* **123**: 228–238.
9. Noble, GT, Stefanick, JF, Ashley, JD, Kiziltepe, T and Bilgicer, B (2014). Ligand-targeted liposome design: challenges and fundamental considerations. *Trends Biotechnol* **32**: 32–45.
10. Le Bihan, O, Chèvre, R, Mornet, S, Garnier, B, Pitard, B and Lambert, O (2011). Probing the *in vitro* mechanism of action of cationic lipid/DNA lipoplexes at a nanometric scale. *Nucleic Acids Res* **39**: 1595–1609.
11. Wasungu, L and Hoekstra, D (2006). Cationic lipids, lipoplexes and intracellular delivery of genes. *J Control Release* **116**: 255–264.
12. Barteau, B, Chèvre, R, Letrou-Bonneval, E, Labas, R, Lambert, O and Pitard, B (2008). Physicochemical parameters of non-viral vectors that govern transfection efficiency. *Curr Gene Ther* **8**: 313–323.
13. White, MB, Amos, J, Hsu, JM, Gerrard, B, Finn, P and Dean, M (1990). A frame-shift mutation in the cystic fibrosis gene. *Nature* **344**: 665–667.
14. Denning, GM, Anderson, MP, Amara, JF, Marshall, J, Smith, AE and Welsh, MJ (1992). Processing of mutant cystic fibrosis transmembrane conductance regulator is temperature-sensitive. *Nature* **358**: 761–764.
15. Colas, J, Faure, G, Saussereau, E, Trudel, S, Rabeh, WM, Bitam, S *et al.* (2012). Disruption of cytokeratin-8 interaction with F508del-CFTR corrects its functional defect. *Hum Mol Genet* **21**: 623–634.
16. Lipecka, J, Norez, C, Bensalem, N, Baudouin-Legros, M, Planelles, G, Becq, F *et al.* (2006). Rescue of DeltaF508-CFTR (cystic fibrosis transmembrane conductance regulator) by curcumin: involvement of the keratin 18 network. *J Pharmacol Exp Ther* **317**: 500–505.
17. Vigneron, JP, Oudrhiri, N, Fauquet, M, Vergely, L, Bradley, JC, Basseville, M *et al.* (1996). Guanidinium-cholesterol cationic lipids: efficient vectors for the transfection of eukaryotic cells. *Proc Natl Acad Sci USA* **93**: 9682–9686.
18. Mével, M, Sainlos, M, Chatin, B, Oudrhiri, N, Hauchecorne, M, Lambert, O *et al.* (2012). Paromomycin and neomycin B derived cationic lipids: synthesis and transfection studies. *J Control Release* **158**: 461–469.
19. Desigaux, L, Sainlos, M, Lambert, O, Chevre, R, Letrou-Bonneval, E, Vigneron, JP *et al.* (2007). Self-assembled lamellar complexes of siRNA with lipidic aminoglycoside derivatives promote efficient siRNA delivery and interference. *Proc Natl Acad Sci USA* **104**: 16534–16539.
20. Zuhorn, IS and Hoekstra, D (2002). On the mechanism of cationic amphiphile-mediated transfection. To fuse or not to fuse: is that the question? *J Membr Biol* **189**: 167–179.
21. Mével, M, Neveu, C, Gonçalves, C, Yaouanc, J-J, Pichon, C, Jaffrès, P-A, *et al.* (2008). Novel neutral imidazole-lipophosphoramides for transfection assays. *Chem Commun Camb Engl* **27**: 3124–3126.
22. Billiet, L, Gomez, J-P, Berchel, M, Jaffrès, P-A, Le Gall, T, Montier, T *et al.* (2012). Gene transfer by chemical vectors, and endocytosis routes of polyplexes, lipoplexes and lipopolyplexes in a myoblast cell line. *Biomaterials* **33**: 2980–2990.
23. Midoux, P, Pichon, C, Yaouanc, J-J and Jaffrès, P-A (2009). Chemical vectors for gene delivery: a current review on polymers, peptides and lipids containing histidine or imidazole as nucleic acids carriers. *Br. J. Pharmacol.* **157**: 166–178.
24. Xu, Y and Szoka, FC (1996). Mechanism of DNA release from cationic liposome/DNA complexes used in cell transfection *Biochemistry (Mosc.)* **35**: 5616–5623.
25. Pitard, B, Oudrhiri, N, Vigneron, JP, Hauchecorne, M, Aguerre, O, Toury, R *et al.* (1999). Structural characteristics of supramolecular assemblies formed by guanidinium-cholesterol reagents for gene transfection. *Proc Natl Acad Sci USA* **96**: 2621–2626.
26. Pack, DW, Hoffman, AS, Pun, S and Stayton, PS (2005). Design and development of polymers for gene delivery. *Nat Rev Drug Discov* **4**: 581–593.
27. Davezac, N, Tondelier, D, Lipecka, J, Fanen, P, Demaugre, F, Debski, J *et al.* (2004). Global proteomic approach unmasks involvement of keratins 8 and 18 in the delivery of cystic fibrosis transmembrane conductance regulator (CFTR)/deltaF508-CFTR to the plasma membrane. *Proteomics* **4**: 3833–3844.
28. Pitard, B, Bello-Roufaï, M, Lambert, O, Richard, P, Desigaux, L, Fernandes, S *et al.* (2004). Negatively charged self-assembling DNA/poloxamine nanospheres for *in vivo* gene transfer. *Nucleic Acids Res* **32**: e159.

This work is licensed under a Creative Commons Attribution-NonCommercial-NoDerivs 4.0 International License. The images or other third party material in this article are included in the article's Creative Commons license, unless indicated otherwise in the credit line; if the material is not included under the Creative Commons license, users will need to obtain permission from the license holder to reproduce the material. To view a copy of this license, visit http://creativecommons.org/licenses/by-nc-nd/4.0/